



Huang, G., Nix, A. R., & Armour, S. M. D. (2008). Decision feedback equalization in SC-FDMA. In IEEE Personal and Indoor Mobile Radio Conference 2008 (PIMRC), Cannes. (pp. 1 - 5). Institute of Electrical and Electronics Engineers (IEEE). 10.1109/PIMRC.2008.4699507

Link to published version (if available):
[10.1109/PIMRC.2008.4699507](https://doi.org/10.1109/PIMRC.2008.4699507)

[Link to publication record in Explore Bristol Research](#)
PDF-document

University of Bristol - Explore Bristol Research

General rights

This document is made available in accordance with publisher policies. Please cite only the published version using the reference above. Full terms of use are available:
<http://www.bristol.ac.uk/pure/about/ebr-terms.html>

Take down policy

Explore Bristol Research is a digital archive and the intention is that deposited content should not be removed. However, if you believe that this version of the work breaches copyright law please contact open-access@bristol.ac.uk and include the following information in your message:

- Your contact details
- Bibliographic details for the item, including a URL
- An outline of the nature of the complaint

On receipt of your message the Open Access Team will immediately investigate your claim, make an initial judgement of the validity of the claim and, where appropriate, withdraw the item in question from public view.

Decision Feedback Equalization in SC-FDMA

Gillian Huang, Andrew Nix and Simon Armour

Centre for Communications Research, University of Bristol
Merchant Venturers Building, Woodland Road, Bristol BS8 1UB, UK
Email: {G.Huang, Andy.Nix, Simon.Armour}@bristol.ac.uk

Abstract—SC-FDMA (Single-Carrier Frequency Division Multiple Access) is employed in the 3GPP LTE (Long-Term Evolution) standard as the uplink transmission scheme. The SC-FDMA signal has a low PAPR. This makes it well-suited to power efficient transmission at the mobile terminal. Although it is a common assumption to use frequency-domain linear equalization in SC-FDMA, a decision feedback equalizer (DFE) composed of a frequency-domain feedforward filter and a time-domain feedback filter can provide enhanced performance. Even when error propagation is taken into account, results show that a DFE still offers a significant performance gain over the conventional LE for uncoded SC-FDMA. This paper demonstrates that SC-FDMA with DFE is capable of increasing the throughput in a power limited channel by up to 41% compared to LE. Alternatively, for a given peak transmit power, the use of a DFE can achieve a 14% coverage extension in NLOS and 19% in LOS.

I. INTRODUCTION

SC-FDMA has been employed in the 3GPP LTE standard as the uplink transmission scheme [1]. The main advantage of SC-FDMA over OFDMA is its lower PAPR (Peak-to-Average Power Ratio) which enables the mobile terminal to achieve more power efficient transmission. Furthermore, simple frequency-domain equalization can be used with the SC-FDMA waveform. SC-FDMA can be seen as an extension of SC-FDE (Single-Carrier Frequency Domain Equalization) [2], with additional flexibility in resource allocation. The 3GPP LTE standard has specified a scalable transmission bandwidth from 1.25MHz to 20MHz. Within the transmission bandwidth, each user can occupy one or more resource blocks (RB, each RB consists of 12 subcarriers) according to the needs of the individual user. Furthermore, the resource allocation can be scheduled dynamically in the frequency domain via channel-dependent scheduling (CDS). This assigns the user to the most favorable frequency resource. The 3GPP LTE standard provides subscribers with a spectrally efficient high data rate service (up to 50Mbps on the uplink), strong QoS (Quality of Service) and power efficient mobile operation [3].

SC-FDMA can be seen as an OFDMA system proceeded by a DFT block. Using the concepts of subcarrier mapping and CDS in the frequency domain, SC-FDMA is often treated much like OFDMA. The use of frequency-domain linear equalization (LE) is a common assumption in SC-FDMA. In OFDMA, the transmit symbols are mapped onto the subcarriers directly in the frequency-domain. Although the frequency-selective channel may result in deep nulls on some subcarriers, the faded subcarriers and frequency-domain equalization do not cause ICI (Inter-Carrier Interference). The ICI is mostly as-

sociated with synchronization error. Note that ICI in OFDMA is equivalent to ISI (Inter-Symbol Interference).

In contrast to OFDMA, SC-FDMA, as its name implies, is a single-carrier system. Frequency-domain LE is an analog to linear transversal equalization in the time domain. Using the ZF (Zero-Forcing) criterion for LE can eliminate the ISI completely, however the large noise enhancement degrades the performance severely. Superior performance can be achieved by using MMSE (Minimum Mean Square Error) criterion that minimizes the MSE of residual-ISI and the filtered noise. However, if MMSE frequency-domain LE is employed in SC-FDMA, the time-domain equalized symbols will still experience some degree of ISI (since an ideal frequency-flat post-equalizer response is never achieved in practice). Although frequency domain LE is simple, it is not the best way to receive a single-carrier waveform such as SC-FDMA.

In this paper a mathematical derivation is provided for the reception of SC-FDMA as a single-carrier transmission. Since SC-FDMA is a single-carrier system, most of the SC equalization algorithms described in [4] can be applied. MLSE (Maximum-Likelihood Sequence Estimation) is known as the optimal SC equalization algorithm. However, its computational complexity grows exponentially with channel delay spread. Furthermore, MLSE is performed purely in the time-domain, so it is not well-suited to SC-FDMA. Decision feedback equalization (DFE) is another solution that performs better than LE due to its ability to cancel postcursor-ISI using previously detected symbols [4]. A DFE structure consisting of an efficient frequency-domain feedforward filter and a time-domain feedback filter for SC-FDE was proposed in [2,5]. In this paper the application of the DFE structure is extended to SC-FDMA.

This paper is organized as follows: Section II provides a mathematical derivation of SC-FDMA as a single-carrier transmission scheme. Section III describes the DFE architecture (and coefficient calculation method) as applied to SC-FDMA. Section IV compares the performance of SC-FDMA using the DFE and LE structures. Section V concludes the paper.

II. MATHEMATICAL DESCRIPTION OF SC-FDMA

In this section, a mathematical derivation is given to express the SC-FDMA transmit and received data symbols as a single-carrier transmission scheme. The use of matrices to describe the functional blocks provides a clear method to understand the system. It is useful in many ways, including analyzing the impact of uplink synchronization errors [6].

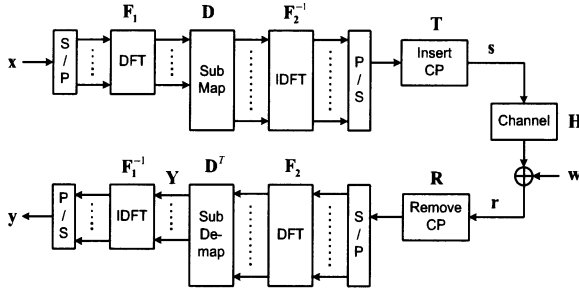


Fig. 1. Block diagram of SC-FDMA system in matrix form

Fig. 1 shows the block diagram of an SC-FDMA system. The transmit data symbols are converted to the frequency domain and the frequency domain symbols are then mapped onto a group of localized or distributed subcarriers. An SC-FDMA symbol is formed after converting back to the time-domain and inserting a CP (cyclic prefix) to construct an SC-FDMA transmission block. The receiver simply performs the inverse process.

As shown in Fig. 1, each function block is represented by a matrix. The transmit SC-FDMA block is denoted as a column vector, $\mathbf{s} = [s_{-P}, \dots, s_0, \dots, s_{N-1}]^T$, where P represents the CP length and N is the total number of available subcarriers (or the IDFT size at the transmitter). The received SC-FDMA block is denoted as $\mathbf{r} = [r_{-P}, \dots, r_0, \dots, r_{N-1}]^T$. Assuming a channel impulse response described as $\{h_l\}_{l=0, \dots, L}$, the received samples in the SC-FDMA block can be represented using (1), where w_i represents the noise term. Equation (1) can also be written in compact matrix form, as shown in (2).

$$r_i = \sum_{l=0}^L h_l s_{i-l} + w_i, \quad i = -P, \dots, N-1 \quad (1)$$

$$\mathbf{r} = \mathbf{H}\mathbf{s} + \mathbf{w} \quad (2)$$

In (2), \mathbf{H} is a $(P+N) \times (P+N)$ channel matrix, denoted as

$$\mathbf{H} = \begin{bmatrix} h_0 & 0 & \cdots & \cdots & \cdots & 0 \\ \vdots & h_0 & \ddots & & & \vdots \\ h_L & \vdots & \ddots & \ddots & & \vdots \\ 0 & h_L & & \ddots & \ddots & \vdots \\ \vdots & \ddots & \ddots & \ddots & \ddots & 0 \\ 0 & \cdots & 0 & h_L & \cdots & h_0 \end{bmatrix}. \quad (3)$$

The transmit data symbols are denoted as $\mathbf{x} = [x_0, \dots, x_{M-1}]^T$ and M represents the number of transmit data symbols in one SC-FDMA block. \mathbf{F}_1 is a $M \times M$ DFT matrix, i.e. $\mathbf{F}_{(p+1, q+1)} = \frac{1}{\sqrt{M}} e^{-j\frac{2\pi}{M}pq}$, where $p, q = 0, \dots, M-1$. \mathbf{F}_2^{-1} is a $N \times N$ IDFT matrix. Note that \mathbf{F}_2^{-1} should have a scaling factor of $\frac{1}{\sqrt{M}}$ instead of $\frac{1}{\sqrt{N}}$ to maintain the same output signal power. \mathbf{D} is a $N \times M$ matrix that maps the m -th user frequency domain symbol onto the n -th available subcarrier, where $m = 0, \dots, M-1$ and $n = 0, \dots, N-1$.

The subcarrier mapping matrix \mathbf{D} for localized and distributed allocations is given in (4) and (5), where RU is the resource unit allocation, $RU = 0, \dots, \frac{N}{M} - 1$.

$$\text{Localized: } \mathbf{D}_{(n+1, m+1)} = \begin{cases} 1, & n = RU.M + m \\ 0, & \text{otherwise} \end{cases} \quad (4)$$

$$\text{Distributed: } \mathbf{D}_{(n+1, m+1)} = \begin{cases} 1, & n = RU + \frac{N}{M}m \\ 0, & \text{otherwise} \end{cases} \quad (5)$$

Hence the transmit SC-FDMA block can be written as (6). The inverse process is performed at the receiver so the received data symbols can be written as (7). Note that at the receiver $\mathbf{Y} = [Y_0, \dots, Y_{M-1}]^T$ denotes the received frequency-domain data symbols, which will be used in Section III.

$$\mathbf{s} = \mathbf{T}\mathbf{F}_2^{-1}\mathbf{D}\mathbf{F}_1\mathbf{x} \quad (6)$$

$$\mathbf{y} = \mathbf{F}_1^{-1}\mathbf{D}^T\mathbf{F}_2\mathbf{R}\mathbf{r} \quad (7)$$

In (6) and (7), \mathbf{T} and \mathbf{R} are defined as

$$\mathbf{T} \triangleq \begin{bmatrix} \mathbf{I}_{CP} \\ \mathbf{I}_N \end{bmatrix}, \quad \mathbf{R} \triangleq \begin{bmatrix} \mathbf{O}_{N \times P} & \mathbf{I}_N \end{bmatrix} \quad (8)$$

where \mathbf{I}_N denotes a $N \times N$ identity matrix. \mathbf{I}_{CP} is a $P \times N$ matrix that copies the last P row of \mathbf{I}_N and $\mathbf{O}_{N \times P}$ is a $N \times P$ zero matrix. By substituting (2) and (6) into (7), the SC-FDMA transmission link can be represented as

$$\mathbf{y} = \mathbf{F}_1^{-1}\mathbf{D}^T\mathbf{F}_2(\mathbf{R}\mathbf{H}\mathbf{T})\mathbf{F}_2^{-1}\mathbf{D}\mathbf{F}_1\mathbf{x} + \mathbf{w}' \quad (9)$$

where $\mathbf{w}' = \mathbf{F}_1^{-1}\mathbf{D}^T\mathbf{F}_2\mathbf{R}\mathbf{w}$ represents the effective noise after receiving process. Equation (9) can be simplified under the matrix associated law. Let $\mathbf{H}_0 = \mathbf{R}\mathbf{H}\mathbf{T}$,

$$\mathbf{H}_0 = \begin{bmatrix} h_0 & 0 & \cdots & 0 & h_L & \cdots & h_1 \\ \vdots & h_0 & \ddots & & \ddots & \ddots & \vdots \\ h_{L-1} & \vdots & \ddots & \ddots & & \ddots & h_L \\ h_L & h_{L-1} & & \ddots & \ddots & & 0 \\ 0 & h_L & \ddots & & \ddots & \ddots & \vdots \\ \vdots & \ddots & \ddots & \ddots & \ddots & \ddots & 0 \\ 0 & \cdots & 0 & h_L & h_{L-1} & \cdots & h_0 \end{bmatrix}. \quad (10)$$

In (10), the circulant matrix \mathbf{H}_0 is formed simply by inserting the CP at the transmitter and removing it at the receiver. A circulant matrix can be diagonalized by pre- and post-multiplication of DFT and IDFT matrices. Hence $\tilde{\mathbf{H}}_0 = \mathbf{F}_2\mathbf{H}_0\mathbf{F}_2^{-1} = \text{diag}\{\tilde{h}_0, \tilde{h}_1, \dots, \tilde{h}_{N-1}\}$ and the diagonal is the channel frequency response, i.e. $\tilde{h}_k = \sum_{l=0}^L h_l e^{-j\frac{2\pi}{N}kl}$.

Furthermore, $\tilde{\mathbf{H}}' = \mathbf{D}^T\tilde{\mathbf{H}}_0\mathbf{D}$ can be defined so that $\tilde{\mathbf{H}}'_{(m+1, m+1)} = \tilde{\mathbf{H}}_{0, (n+1, n+1)}$, where the equation of m and n is specified in (4) and (5) depending on the subcarrier mapping mode. Therefore $\tilde{\mathbf{H}}'$ is also a diagonal matrix, i.e. $\tilde{\mathbf{H}}' = \text{diag}\{\tilde{h}'_0, \tilde{h}'_1, \dots, \tilde{h}'_{M-1}\}$ and the diagonal represents the channel frequency response on the user subcarriers. The diagonal matrix $\tilde{\mathbf{H}}'$ can be decomposed into a multiplication of a DFT matrix, a circulant matrix and an IDFT matrix, i.e.

$\tilde{\mathbf{H}}' = \mathbf{F}_1 \mathbf{H}' \mathbf{F}_1^{-1}$. Now (9) can be reduced to (11), to show the SC-FDMA transmit and received data symbol as a single-carrier transmission.

$$\mathbf{y} = \mathbf{F}_1^{-1} (\mathbf{F}_1 \mathbf{H}' \mathbf{F}_1^{-1}) \mathbf{F}_1 \mathbf{x} + \mathbf{w}' = \mathbf{H}' \mathbf{x} + \mathbf{w}' \quad (11)$$

In (11), \mathbf{H}' is a circulant matrix that represents the 'resultant channel impulse response' between the transmit and received SC-FDMA data symbols. This resultant channel impulse response can be obtained by converting the channel frequency response on the user subcarriers to the time-domain,

$$h'_l = \frac{1}{M} \sum_{k=0}^{M-1} \tilde{h}'_k e^{j \frac{2\pi}{M} kl}, \quad l = 0, \dots, L'. \quad (12)$$

Therefore (11) can also be written as

$$y_m = \sum_{l=0}^{L'} h'_l x_{m-l} + w'_m, \quad m = 0, \dots, M-1 \quad (13)$$

and $x_p = x_{p+M}$ for $-P \leq p \leq -1$ since the CP processing forces the linear convolution of the channel with the transmit signal to appear as a cyclic convolution. It is shown in (13) that SC-FDMA is indeed a single-carrier system, so it follows that SC equalization algorithms are applicable.

Note that in (12), converting the channel frequency response on the localized subcarriers back to the time-domain results in a down-sampling effect on the original channel impulse response. Hence the resultant channel memory can be orders of magnitude shorter than the original channel memory. This can be estimated as $L' = \text{ceil}[(L+1) \times \frac{M}{N}] - 1$. However, converting the channel frequency response on the distributed subcarriers to the time-domain results in the reconstruction of the original channel impulse response. Hence the length of the resultant channel memory remains the same, i.e. $L' = L$.

III. SC-FDMA WITH DFE

The MMSE-DFE minimizes the MSE of residual precursor-ISI and the filtered noise (assuming postcursor-ISI can be completely removed by the feedback filter). Hence the DFE provides better performance than the MMSE-LE. The DFE algorithm used in this paper for SC-FDMA is based on [5]. The derivation of the coefficient calculation is given in [5], and hence here only the results are shown.

The received symbol y_m in (13) is the unequalized time-domain symbol, with ISI spanning a number of previous time-domain symbols. Y_k (see Fig. 1) is the unequalized frequency-domain data symbol, i.e. $Y_k = \frac{1}{\sqrt{M}} \sum_{m=0}^{M-1} y_m e^{-j \frac{2\pi}{M} mk}$, which can be equalized using the DFE. Fig. 2 shows the DFE structure for a SC-FDMA receiver consists of a frequency-domain feedforward (FF) filter, G_{FF} , and a time-domain feedback (FB) filter, g_{FB} . \hat{x}_m denotes the hard-decision feedback symbols, and \tilde{x}_m denotes the decision-feedback equalized symbols. Hence the DFE process can be described as

$$\tilde{x}_m = \frac{1}{M} \sum_{k=0}^{M-1} (G_{FF,k} Y_k) e^{j \frac{2\pi}{M} km} - \sum_{l=1}^{N_{FB}} g_{FB,l} \hat{x}_{m-l}, \quad m = 0, \dots, M-1. \quad (14)$$

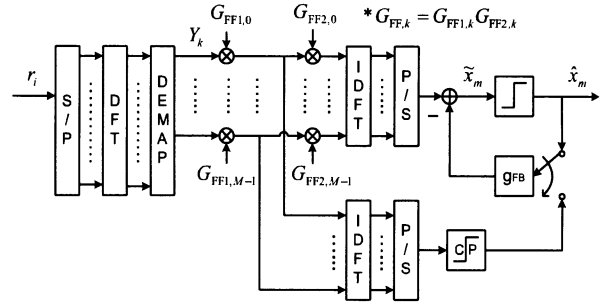


Fig. 2. DFE structure for SC-FDMA systems

The length of the feedback (FB) filter is set to match the length of the resultant channel memory to ensure that all the ISI from the previous symbols are cancelled, i.e. $N_{FB} = L'$. Note that for distributed FDMA (DFDMA) this may require a longer N_{FB} compared to localized FDMA (LFDMA).

The FB coefficients can be obtained by solving the linear equation, $\mathbf{A}_{MMSE} \mathbf{g}_{FB} = \mathbf{b}_{MMSE}$. The matrix \mathbf{A}_{MMSE} and the column vector \mathbf{b}_{MMSE} are given by

$$[\mathbf{A}_{MMSE}]_{i,l} = \sum_{k=0}^{M-1} \frac{e^{-j \frac{2\pi}{M} k(l-i)}}{|\tilde{h}'_k|^2 + \frac{\sigma_w^2}{\sigma_x^2}}, \quad 1 \leq i, l \leq L' \quad (15)$$

$$[\mathbf{b}_{MMSE}]_i = - \sum_{k=0}^{M-1} \frac{e^{j \frac{2\pi}{M} ki}}{|\tilde{h}'_k|^2 + \frac{\sigma_w^2}{\sigma_x^2}}, \quad 1 \leq i \leq L' \quad (16)$$

where \tilde{h}'_k denotes the channel frequency response on the k -th user subcarrier and $\frac{\sigma_w^2}{\sigma_x^2}$ is the signal-to-noise ratio. The FF coefficients are

$$G_{FF,k} = \left(\frac{(\tilde{h}'_k)^*}{|\tilde{h}'_k|^2 + \frac{\sigma_w^2}{\sigma_x^2}} \right) \times (1 + G_{FB,k}) \quad (17)$$

where $(\cdot)^*$ denotes the complex conjugation. Let $G_{FF1,k}$ be the first term in (17). This is equivalent to the MMSE-LE. $G_{FF1,k}$ can be used to obtain the last N_{FB} symbols in the received block as the initial FB symbols, as shown in Fig. 2. The FF filter is completed by $G_{FF2,k}$, the second term in (17), where $G_{FB,k} = \sum_{l=1}^{N_{FB}} g_{FB,l} e^{-j \frac{2\pi}{M} kl}$, $k = 0, \dots, M-1$. In addition, the MMSE solution will reduce to the ZF solution if $\sigma_w^2 = 0$.

IV. SIMULATION RESULTS

This section presents a comparison of the simulation results for the LE and DFE in the case of SC-FDMA. In the simulation, it is assumed that the subcarrier bandwidth is 15kHz [1], the total number of available subcarriers $N = 512$ and the number of user subcarriers $M = 128$. The CP length is $P = 64$ which is longer than the channel delay spread. Hence one SC-FDMA block period is now $T_{BLK} = (512 + 64)/(15\text{kHz} \times 512) = 75\mu\text{s}$. The urban macro scenario as defined in the SCME (Spatial Channel Model Extended) [7,8] is used in the simulation. Ideal channel estimation is assumed.

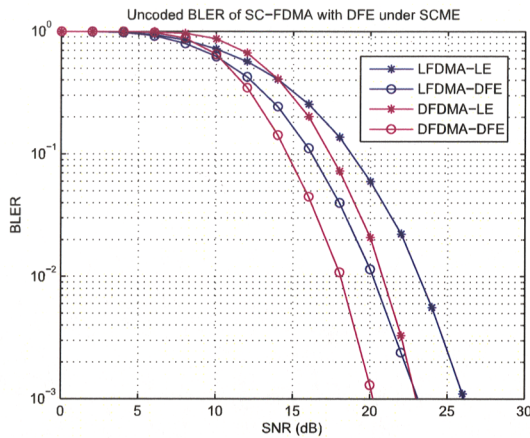


Fig. 3. Uncoded BLER of LFDMA and DFDMA with DFE

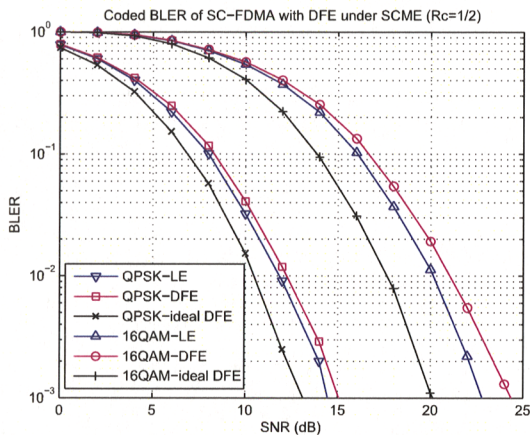


Fig. 4. Coded BLER of SC-FDMA with DFE

When channel coding is applied, a 1/2-rate convolutional encoder (133,171) followed by a block interleaver is used at the transmitter and a block de-interleaver followed by a soft-decision Viterbi decoder is used at the receiver. The feedback decisions used in the DFE are generated from the previous hard-decision detected symbols. Hence, the impact of error propagation is included in the model.

Fig. 3 shows the uncoded BLER (Block Error Rate) of LFDMA and DFDMA using the DFE. Even with error propagation, the DFE shows around 3dB of gain over the LE (at a BLER=0.01). DFDMA provides a better BLER performance due to its frequency diversity. However, the frequency diversity gain in DFDMA is overwhelmed by the large performance loss of real channel estimation [9], and it is no longer supported in the 3GPP LTE standard [10]. All subsequent simulation results are therefore based on LFDMA.

Fig. 4 shows that the coded BLER performance using the DFE is slightly worse than the LE. This can be explained by the CDF (Cumulative Distribution Function) of the bit

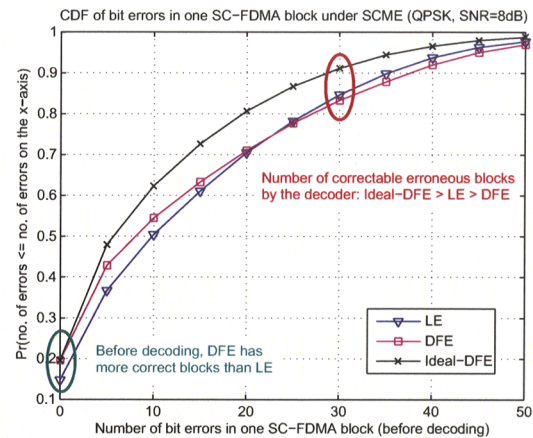


Fig. 5. CDF of bit errors in one SC-FDMA block before decoding

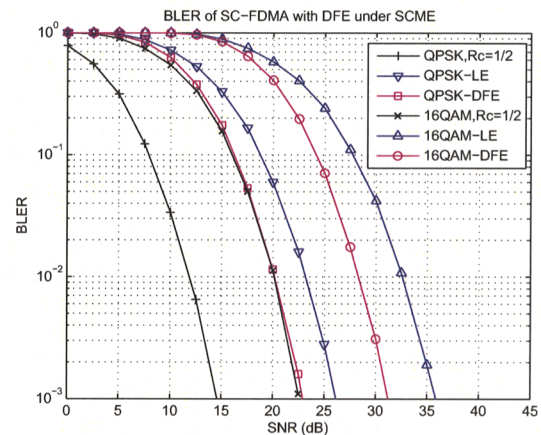


Fig. 6. BLER comparison of coded-LE and uncoded-DFE for SC-FDMA

error distribution in one SC-FDMA block before decoding, as shown in Fig. 5. From analyzing the decoder output, it is observed that it is unlikely for the decoder to correct an erroneous block which has more than 30 bit errors before the decoding process. Although the DFE has more error-free blocks than the LE prior to decoding, more erroneous blocks in the LE can be corrected by the decoder and hence the coded BLER is better than the DFE.

Fig. 5 also shows the ideal-DFE (i.e. assume perfect feedback decision, no error propagation) has more correctable erroneous blocks than the LE and yields a significant gain over the LE, as shown in Fig. 4. It can be concluded that there is a large performance loss in the DFE due to error propagation when coding is applied. Various methods have been proposed to tackle error propagation in the DFE [11-13]. Further work is required to improve this aspect of the design.

Fig. 6 shows the BLER comparison of the coded-LE and the uncoded-DFE. The DFE gain over the LE is larger when higher level modulation is used. The DFE results in around

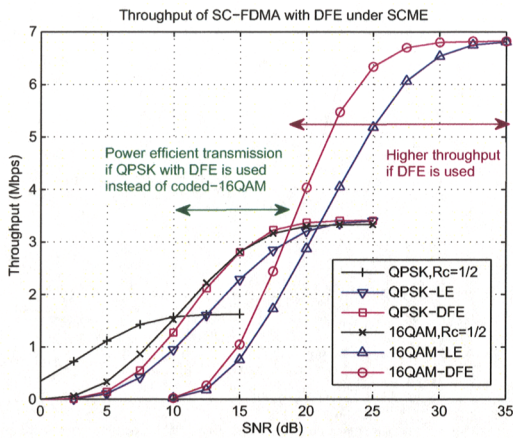


Fig. 7. Throughput comparison of SC-FDMA with LE and DFE

5dB of gain (at a BLER=0.01) over the LE for uncoded 16QAM. Uncoded-QPSK with the DFE has almost the same BLER as coded-16QAM using the LE (Note: uncoded QPSK and 1/2-rate 16QAM have the same data rate). Fig. 7 shows the throughput results obtained using the graphs shown in Fig. 6. The throughput can be estimated as $(1 - \text{BLER}) \times \frac{N_{\text{bits}}}{T_{\text{BLK}}}$, where N_{bits} denotes the number of information bits in one block.

Two remarkable results for SC-FDMA using a DFE are shown in Fig. 7. One is the significant throughput enhancement of uncoded 16QAM at high SNR. For example, there is a 41% of throughput enhancement achieved by the DFE compared to the LE at an SNR of 20dB. The other is that uncoded-QPSK with the DFE and 1/2-rate 16QAM with the LE achieve almost the same throughput for SNR in the range 10 to 18dB. Since QPSK has a lower PAPR than 16QAM, it is more power efficient for the mobile terminal to transmit uncoded-QPSK if a DFE is used at the BS (basestation).

Furthermore, Fig. 8 shows that $\pi/4$ -QPSK (which has the same error performance as QPSK but with lower PAPR) has a 2dB lower PAPR than 16QAM if RRC (root raised cosine) frequency domain spectrum shaping is employed with a small roll-off factor of 0.2. If the peak transmit power at the mobile terminal is fixed, $\pi/4$ -QPSK requires less backoff than 16QAM and hence the mean transmit power can be increased. This translates to improved coverage without sacrificing throughput. For example, a 2dB improvement in the mean transmit power translates to a 14% improvement in coverage for NLOS (Non Light-of-Sight) locations (based on the SCME urban macro pathloss model [7] and a pathloss exponent of 3.5). In the LOS case with the pathloss exponent of 2.6 [7], the coverage extension increases to 19%.

V. CONCLUSIONS

This paper demonstrates the benefits of using a DFE to receive SC-FDMA. A DFE gives better performance than a LE due to its ability to cleanly remove past echo ISI. Since increased complexity is viable at the BS, SC-FDMA with DFE

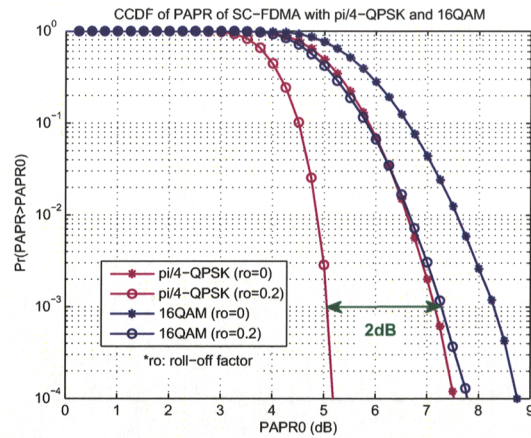


Fig. 8. PAPR of $\pi/4$ -QPSK and 16QAM with/without RRC spectrum shaping

reception can be considered for use on the uplink of 3GPP LTE to increase throughput and to achieve more power efficient transmission (or coverage extension). When coding is applied, the error propagation problem in the DFE lowers performance, and this is the subject of further study.

REFERENCES

- [1] 3GPP, "Physical Layer Aspects for Evolved UTRA," TR 25.814 V7.1.0, Sept. 2006. [online]. Available: <http://www.3gpp.org/ftp/Specs/html-info/25814.htm>.
- [2] D. Falconer *et al.*, "Frequency Domain Equalization for Single-Carrier Broadband Wireless Systems," *IEEE Commun. Mag.*, vol. 40, no. 4, pp. 58-66, Apr. 2002.
- [3] 3GPP, "Requirements for Evolved UTRA (E-UTRA) and Evolved UTRAN (E-UTRAN)," TR 25.913 V7.3.0, Mar. 2006. [online]. Available: <http://www.3gpp.org/ftp/Specs/html-info/25913.htm>.
- [4] J. G. Proakis, *Digital Communications*, 4th ed. New York: McGraw-Hill, 2001.
- [5] N. Benvenuto and S. Tomasin, "On the Comparison between OFDM and Single-Carrier Modulation with a DFE Using a Frequency-Domain Feedforward Filter," *IEEE Trans. Commun.*, vol. 50, no. 6, pp. 947-955, Jun. 2002.
- [6] Z. Cao *et al.*, "Frequency Synchronization for Generalized OFDMA Uplink," in *Proc. Globecom '04*, vol. 2, pp. 1071-1075, Dallas, Nov. 2004.
- [7] D. Baum *et al.*, "An Interim Channel Model for Beyond-3G System: Extending the 3GPP Spatial Channel Model," in *Proc. VTC '04-Spring*, vol. 5, Stockholm, May. 2005.
- [8] D. Baum *et al.*, "MATLAB Implementation of the Interim Channel Model for Beyond-3G Systems (SCME)," May 2005. [online]. Available: <http://www.tkk.fi/Units/Radio/scm>.
- [9] NEC Group, "Further Results for Distributed FDMA and Localized FDMA with Frequency Hopping for EUTRA Uplink," 3GPP, R1-051355, Seoul, Korea, Nov. 2005.
- [10] 3GPP TSG RAN WG1 Meeting Report#47, R1-063613, pp.16, Latvia, Nov. 2006.
- [11] E. Dahlman and B. Gudmundson, "Performance Improvement in Decision Feedback Equalizer by using 'Soft-Decision'," *Electron. Lett.*, vol. 24, no. 17, pp. 1084-1085, Aug. 1988.
- [12] J. W. M. Bergmans, J. O. Voorman and H. W. Wong-Lam, "Dual Decision Feedback Equalizer," *IEEE Trans. Commun.*, vol. 45, no. 5, pp. 514-518, May 1997.
- [13] C. Beare, "The Choice of Desired Impulse Response in Combined Linear-Viterbi Algorithm Equalizers," *IEEE Trans. Commun.*, vol. 26, no. 8, pp. 1301-1307, Aug. 1978.